



Gold, Silver Magnesium and Magnetic Nanoparticles: Nanomedicine Applications in Drug Delivery

Mauro Comes Franchini

***Department of Industrial Chemistry «Toso Montanari»
(School of Sciences, University of Bologna, Italy)***

***4th International Conference on Nanotek & Expo
December 01-03, 2014, San Francisco, USA***

ALMA MATER STUDIORUM - UNIVERSITÀ DI BOLOGNA

IL PRESENTE MATERIALE È RISERVATO AL PERSONALE DELL'UNIVERSITÀ DI BOLOGNA E NON PUÒ ESSERE UTILIZZATO AI TERMINI DI LEGGE DA ALTRE PERSONE O PER FINI NON ISTITUZIONALI



THERANOSTIC NANOMEDICINE

THERANOSTICS

THERAPY

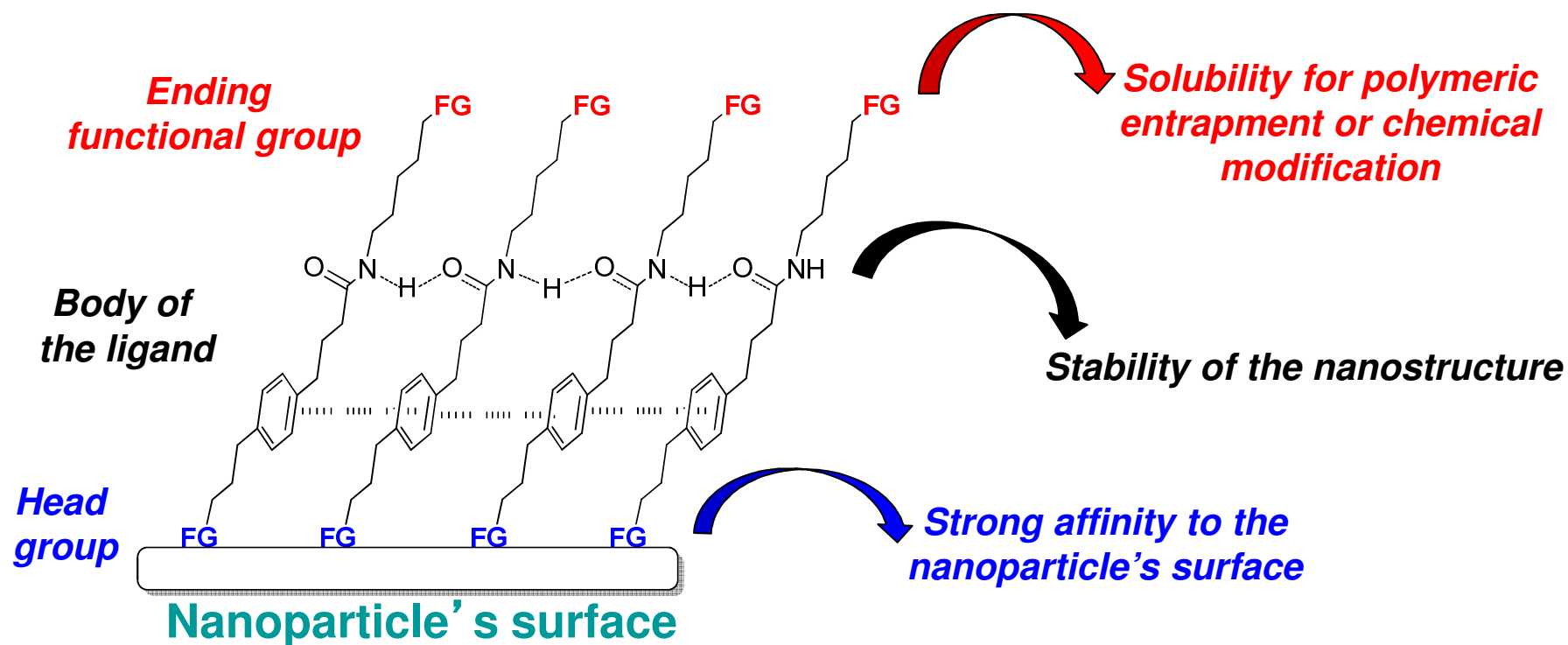
DIAGNOSTICS

**DRUG DELIVERY
HYPEROTHERMIA**

IMAGING



Organic chemistry for nanotechnologies



Introduction to Nanoscience.

G. L. Hornyak. Taylor and Francis Group, 2008



Outline

1. Synthesis of metallic nanoparticles (NPs). Organic ligands to coat the metallic NPs (ligand exchange): lipophilic metallic NPs.

2. Polymeric nanoparticle' s (PNPs) formation. Chemical conjugation in the outer shell of the PNPs. The active targeting.

3. Theranostics: *In vitro* and *In vivo* applications.

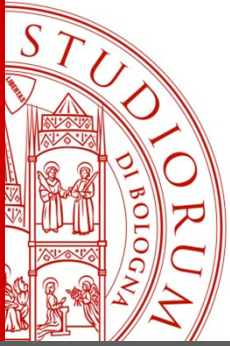


Outline

1. Synthesis of metallic nanoparticles (NPs). Organic ligands to coat the metallic NPs (ligand exchange): lipophilic metallic NPs.

2. Polymeric nanoparticle's (PNPs) formation. Chemical conjugation in the outer shell of the PNPs. The active targeting.

3. Theranostics: *In vitro* and *In vivo* applications.



Magnetic Nanoparticles

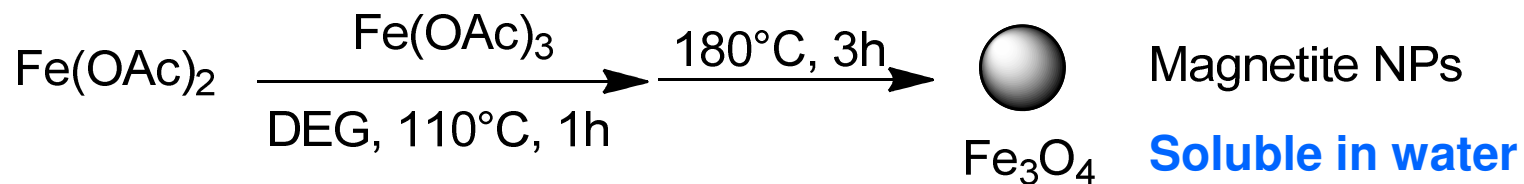


Applications:

Diagnosis MRI, and Therapy using Magnetic Fluid Hyperthermia (MFH) to kill/burn cells.

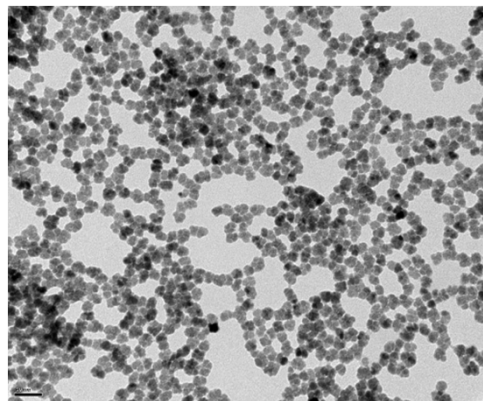


Synthesis of the monodispersed Fe_3O_4 NPs via polyol method

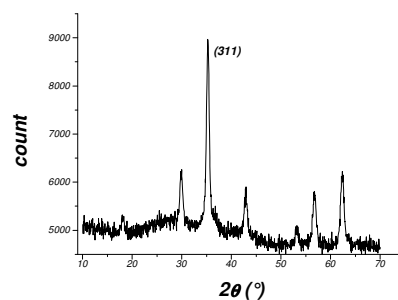


Uniform dispersion of nanoparticles with mean diameter of 23.2 nm.

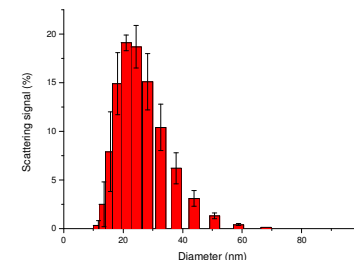
Nanoparticles stable for over one year.



TEM



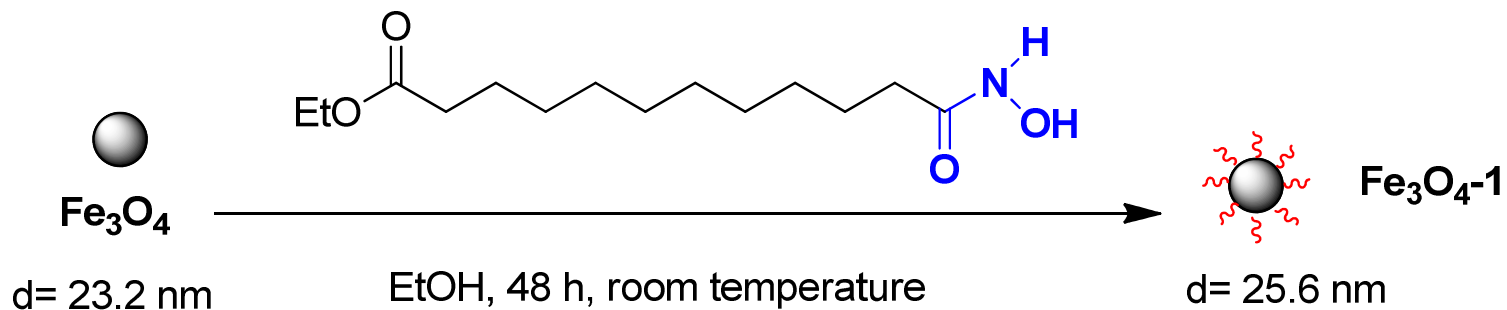
X-ray



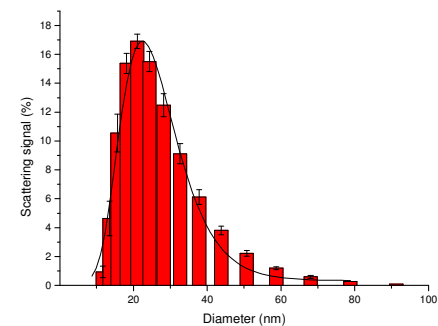
DLS



The Ligand exchange procedures

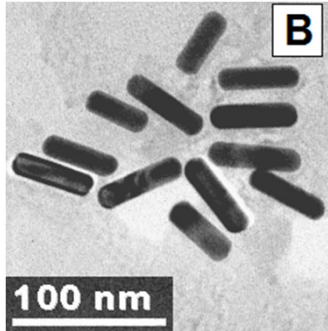


Soluble in THF, DMF, CHCl_3





Gold Nanorods (GNRs)

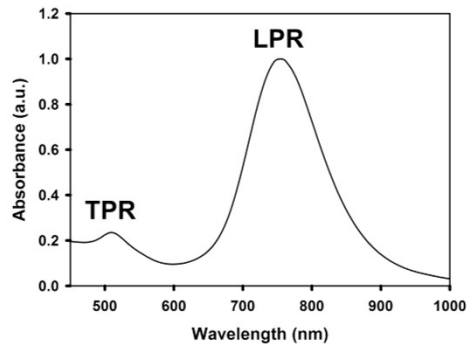


Applications:
Photo-thermal therapy and several
techniques for imaging

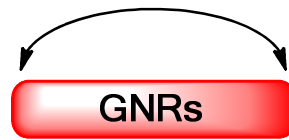


Plasmonic gold nanostructures: Gold Nanorods (GNRs)

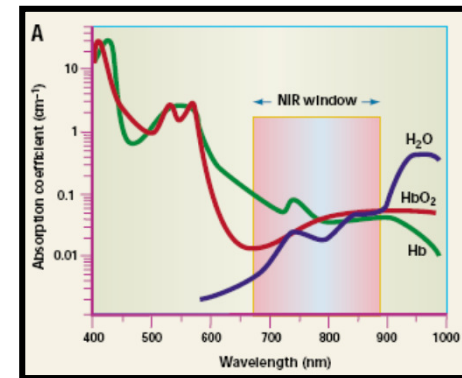
GNRs possess two absorption bands tunable by changing their **aspect ratio**.



Longitudinal plasmon resonance (LPR)



Transversal plasmon resonance (TPR)



R. Weissleder, *Nature Biotechnol.*, **2001**, 19, 316.

For *in vivo* applications, it is desirable to work in the **near-infrared (NIR)** region (750-900 nm), due to the low absorption of tissues in this window.

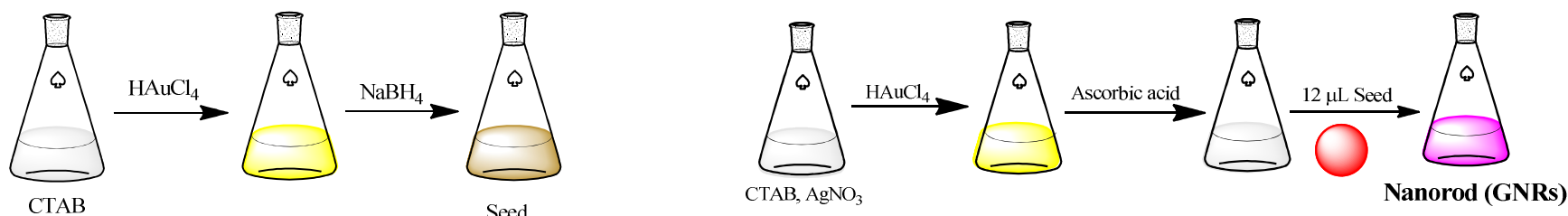
Biocompatibility and unique responses under stimuli allow GNRs use as contrast agents, for instance in **optoacoustic imaging**

High capacity in absorbing radiation and in converting it into heat allows localized **hyperthermia therapy** for cancer cells destruction

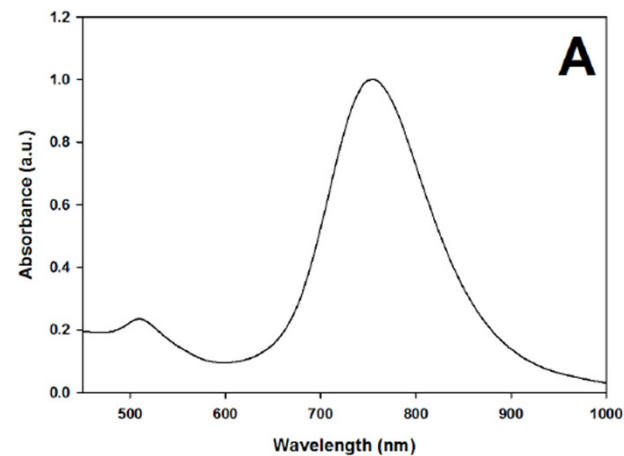
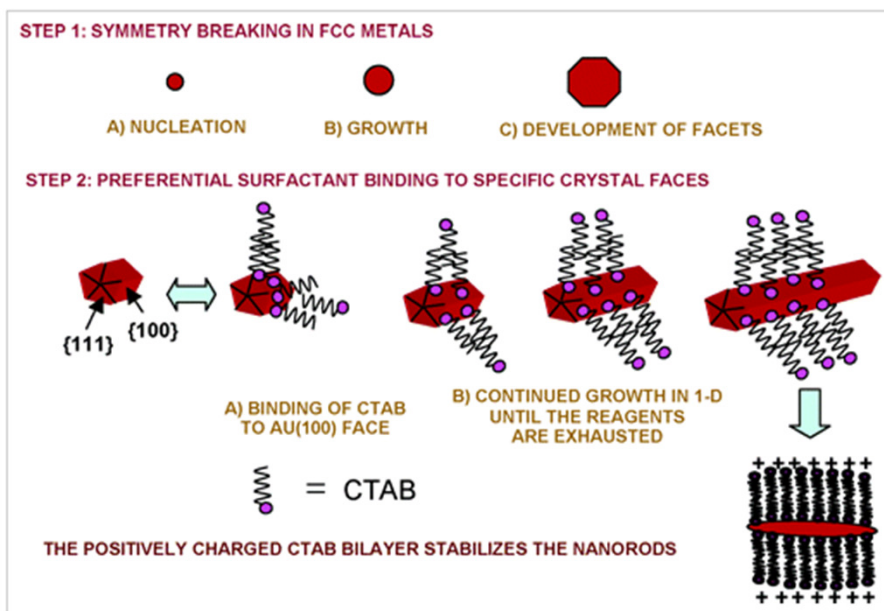
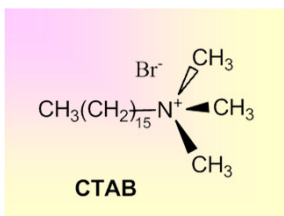


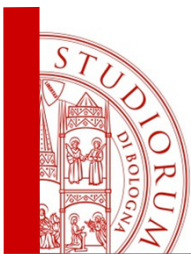
Synthesis of Gold Nanorods

Template-assisted seed-mediated growth.....



GNRs-CTAB-1





The Ligand exchange procedures

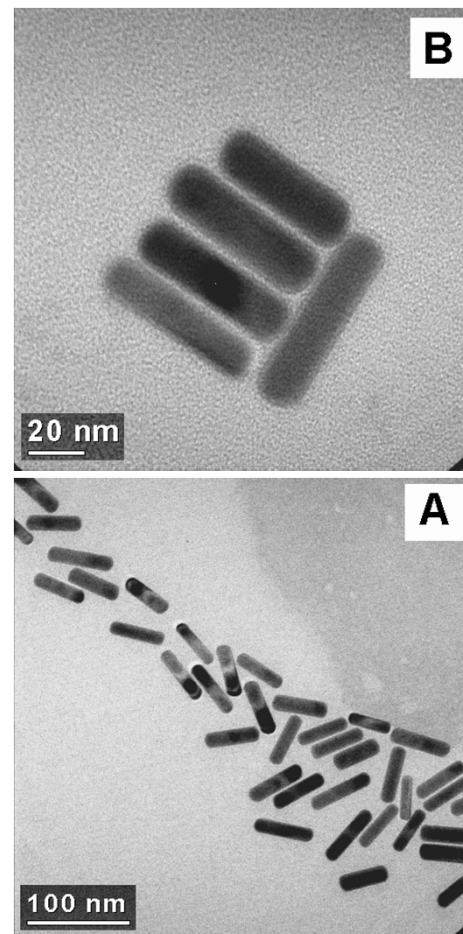
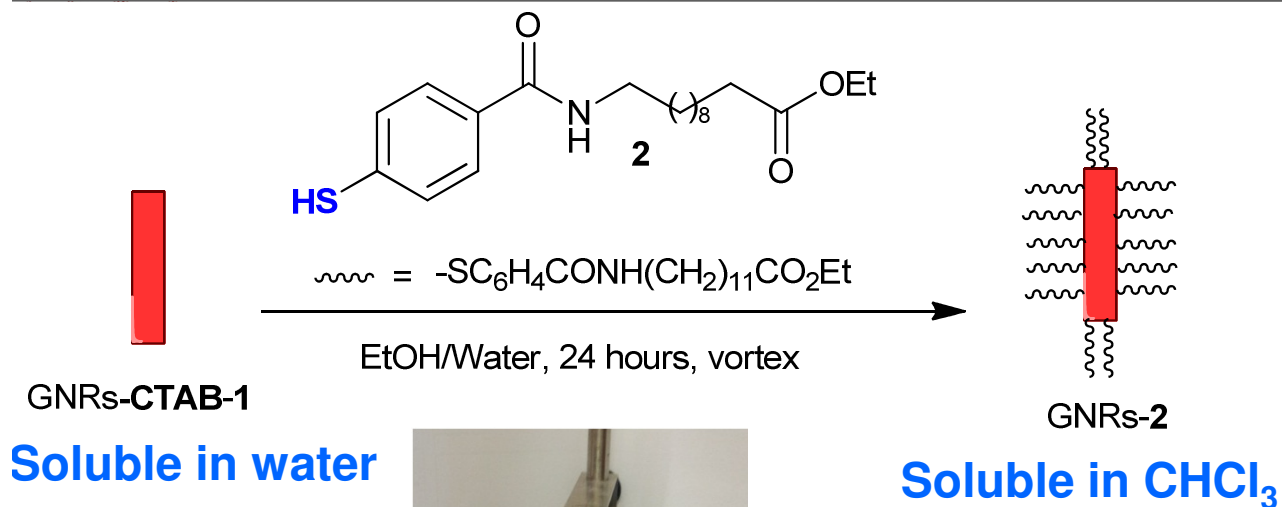
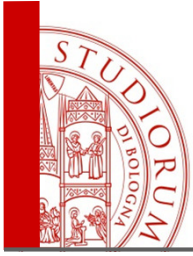
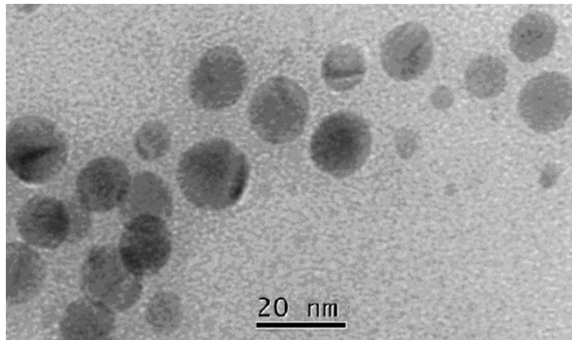


Figure S7. HRTEM (A and B) of GNRs-2.



Silver Nanoparticles



Applications:
Bactericidal properties and
drug-like cytotoxicity

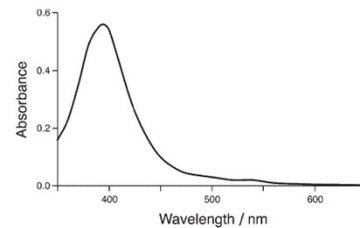


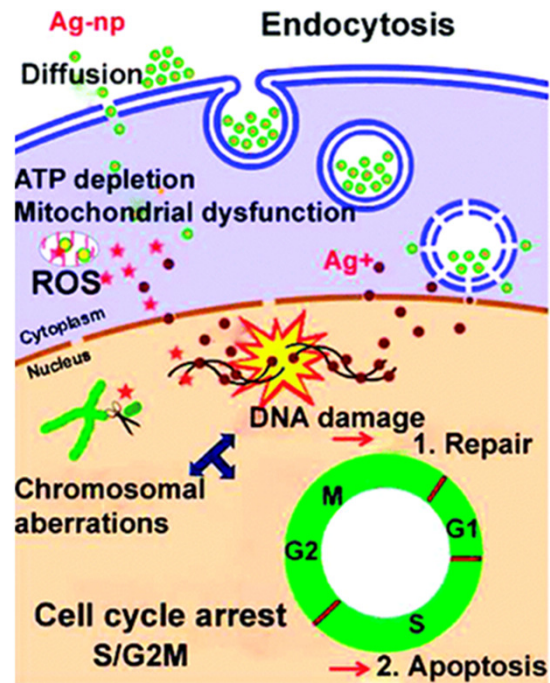
Figure 2. UV-vis absorption spectrum of clear yellow colloidal Ag.





Cytotoxic properties of Ag NPs

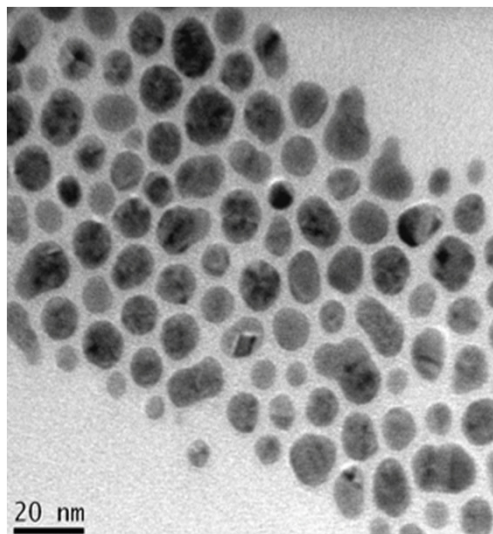
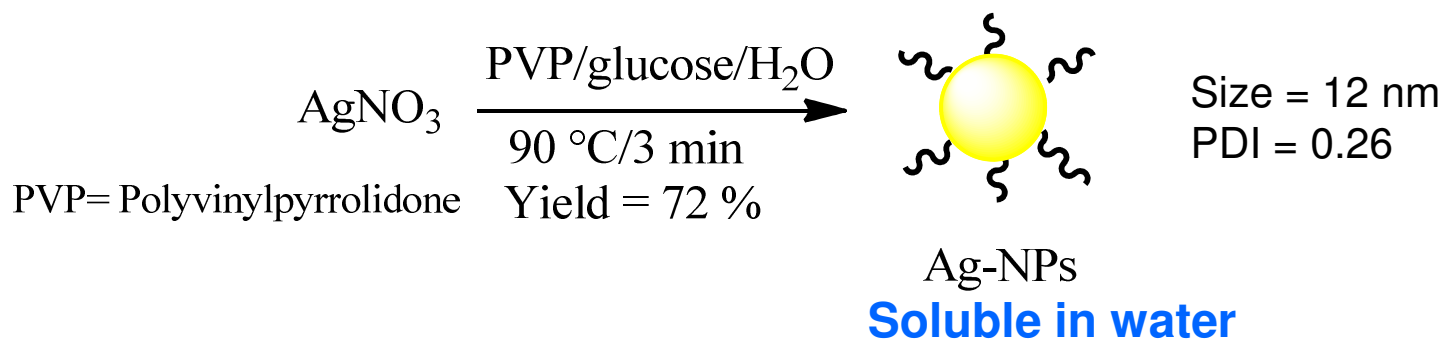
The bactericidal and bacteriostatic properties of spherical Ag NPs have been well known for sometime. Recently, **Ag NPs have also attracted a great deal of attention in biomedical applications due to their toxicity on cell membranes.**



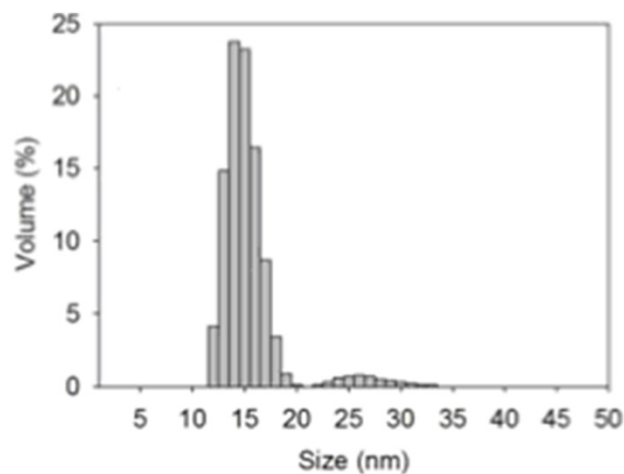
S. K. Gogoi; P. Gopinath; A. Paul; A. Ramesh; S. S. Ghosh; A. Chattopadhyay. *Langmuir*, **2006**, 22, 9322.



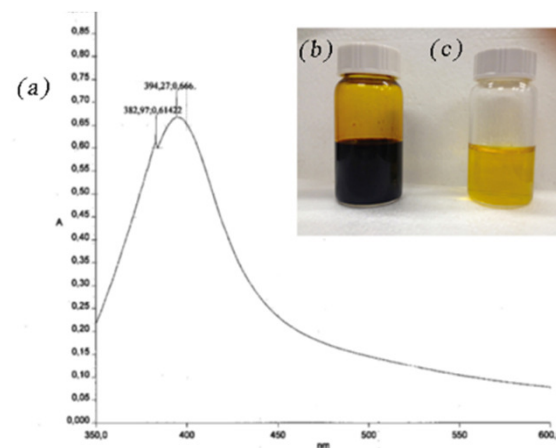
Synthesis of Silver Nanoparticles



TEM



DLS



UV-VIS



The Ligand exchange procedures

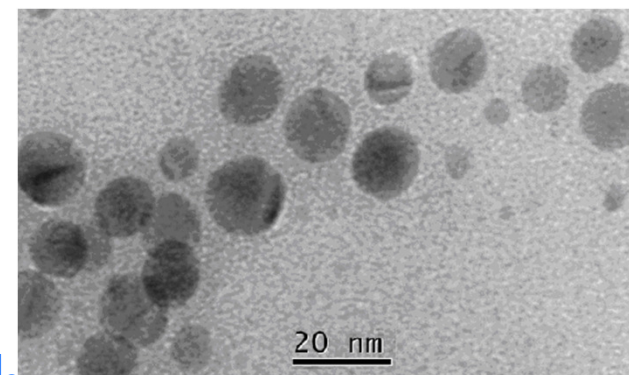
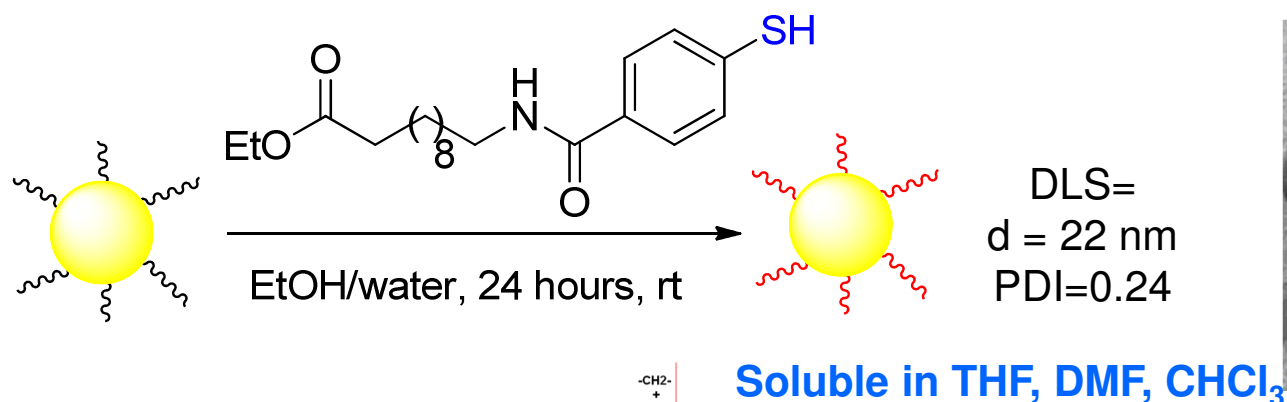


Figure S3. TEM of AgNPs-1.

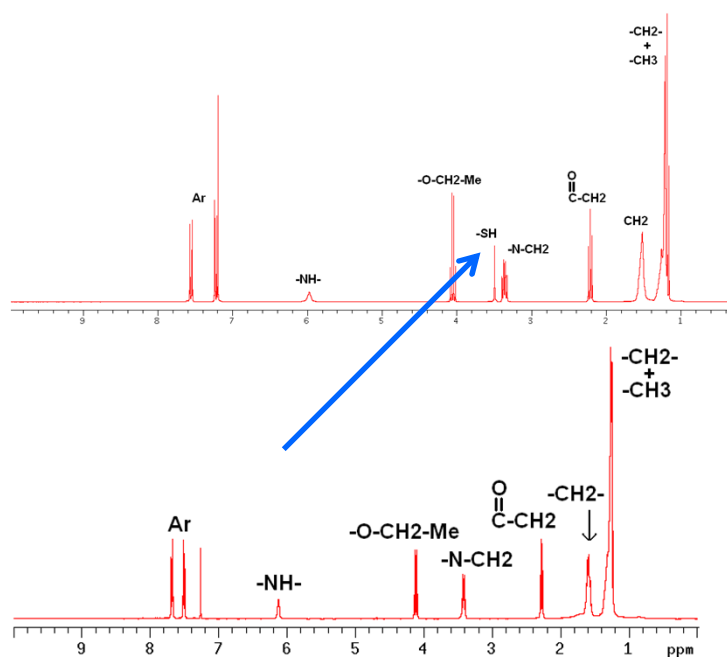


Figure S4. ¹H-NMR of ligand 1 (top) and AgNPs-1 (down)

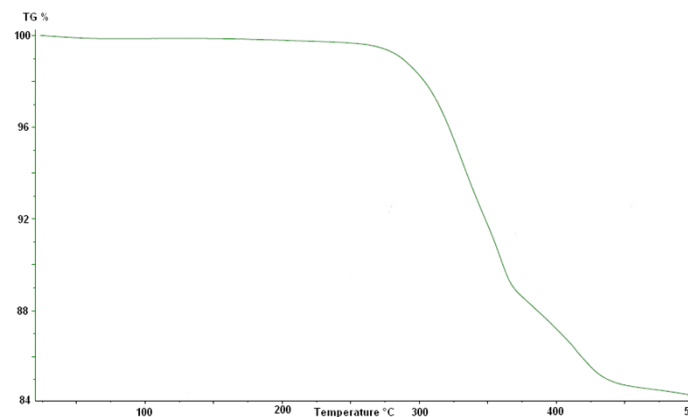


Figure S5. TGA of AgNPs-1



Outline

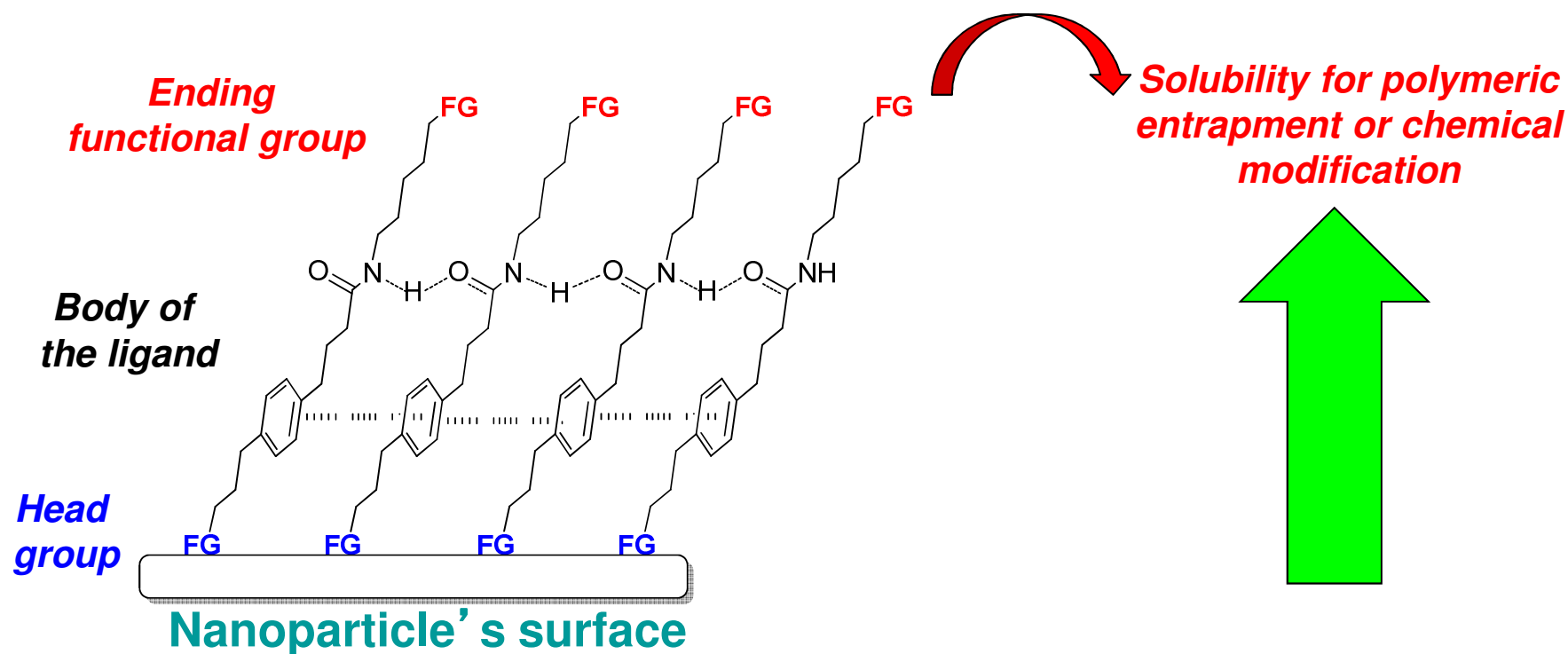
1. Synthesis of metallic nanoparticles (NPs). Organic ligands to coat the metallic NPs (ligand exchange): lipophilic metallic NPs.

2. Polymeric nanoparticle' s (PNPs) formation. Chemical conjugation in the outer shell of the PNPs. The active targeting.

3. Theranostics: *In vitro* and *In vivo* applications.



Organic chemistry for nanotechnologies

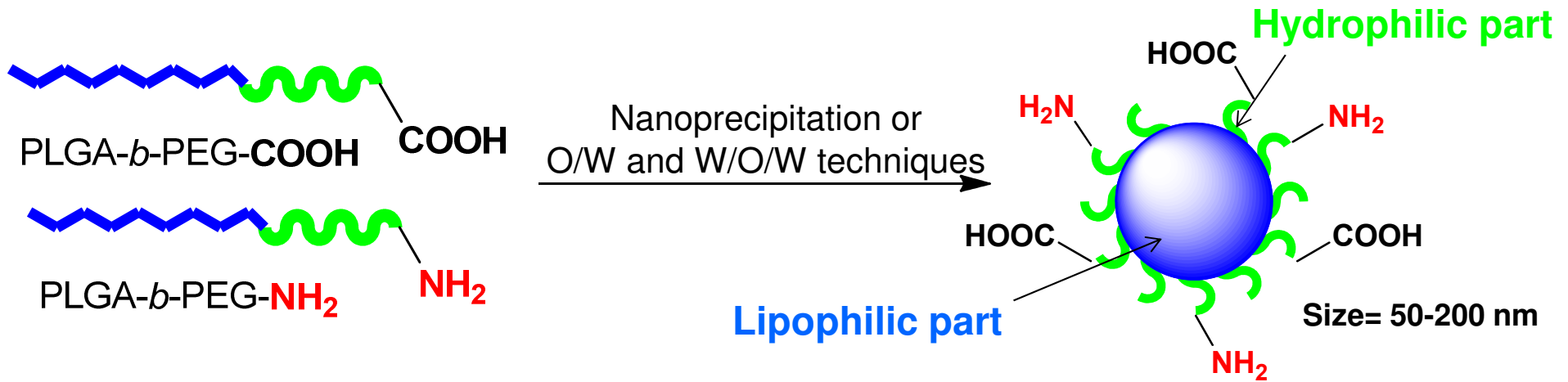


Introduction to Nanoscience.

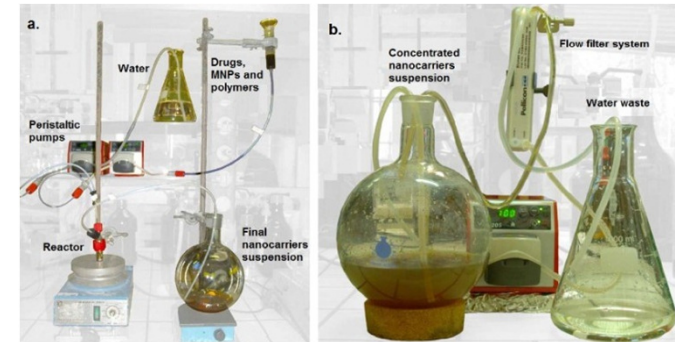
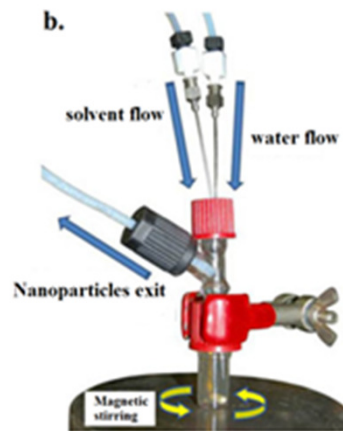
G. L. Hornyak. Taylor and Francis Group, 2008



Polymeric nanoparticle's (PNPs) formation



Tip-sonicator for the Oil/water technique



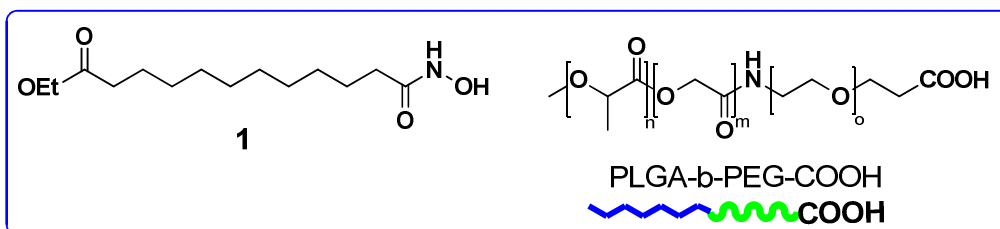
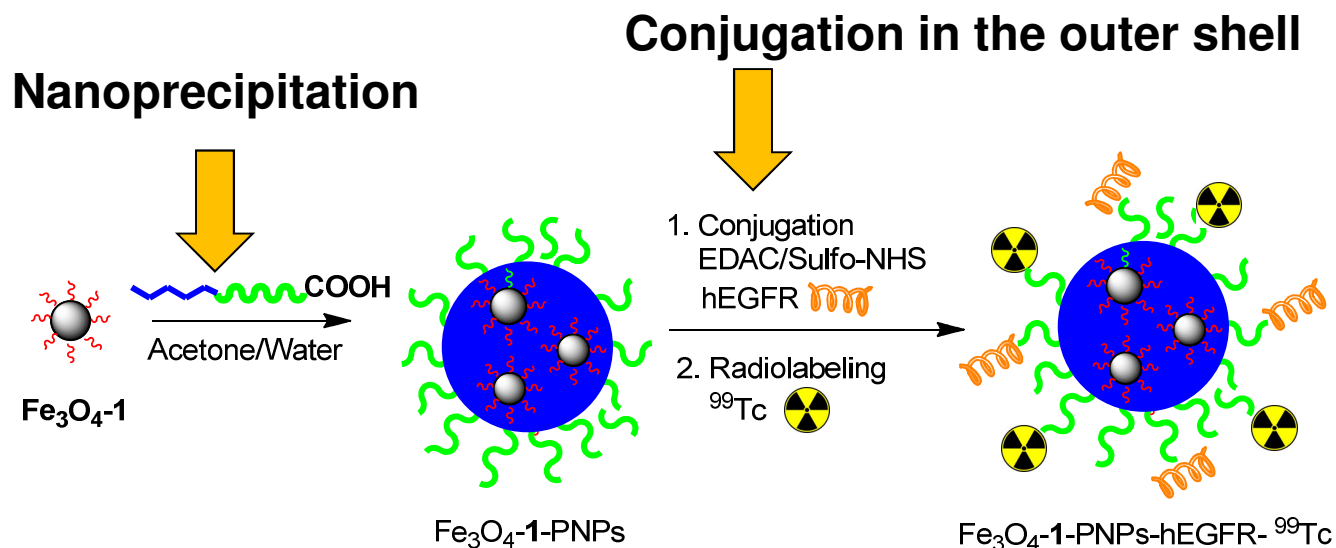
Flow-chemistry for nano-precipitation technique and separation



Magnetic Nanoparticles

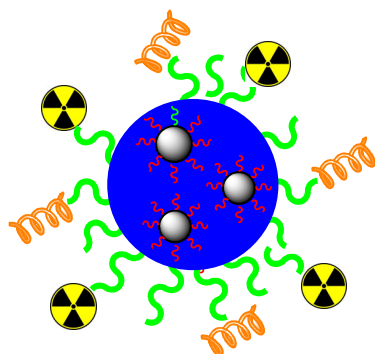


In vivo Anti-Cancer Evaluation of Hyperthermic Efficacy of anti-hEGFR-Targeted PEG-based Nanocarrier Containing Magnetic Nanoparticles



These **hybrid nanoparticles have been targeted with a monoclonal antibody (MoAb) in epidermoid carcinoma (A431)** animal mouse models and radiolabelled with the γ -photon emitting radionuclide Technetium ($^{99\text{m}}\text{Tc}$).

Characterization



Fe_3O_4 -1-PNPs-*h*EGFR- ^{99}Tc

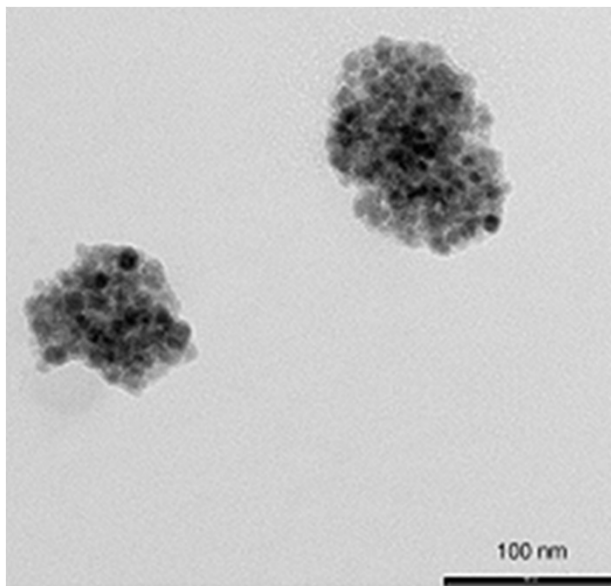
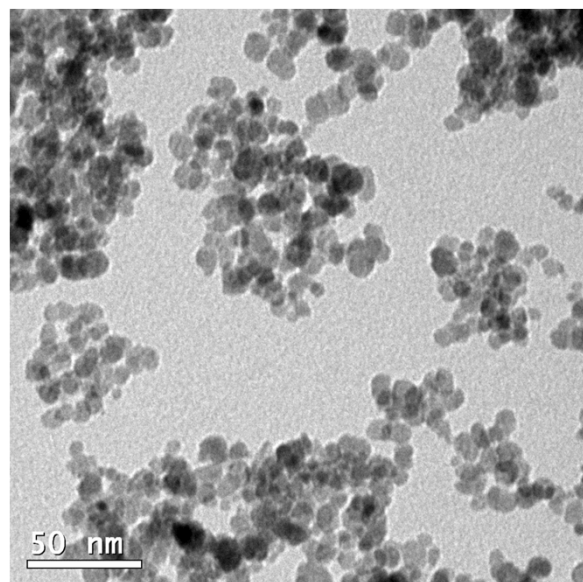
DLS: $d = 101.1 \pm 5.2 \text{ nm}$

$\text{PDI} = 0.218 \pm 0.061$

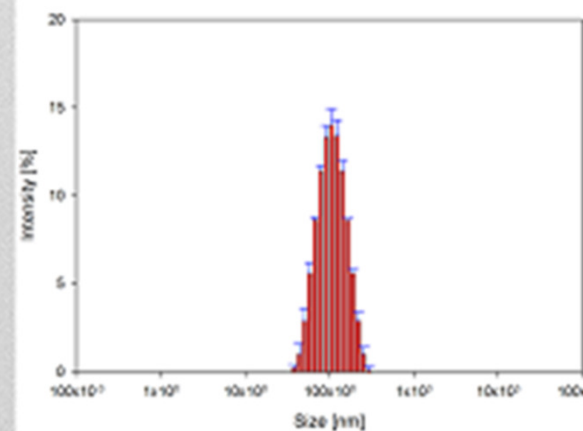
$\zeta_{\text{pot}} = -33.3 \pm 8.0 \text{ mV}$

ICP: $[\text{Fe}] = 0.233 \pm 0.138 \text{ mg/mL}$

Dry matter = $9.21 \pm 0.81 \text{ mg/mL}$



TEM and DLS

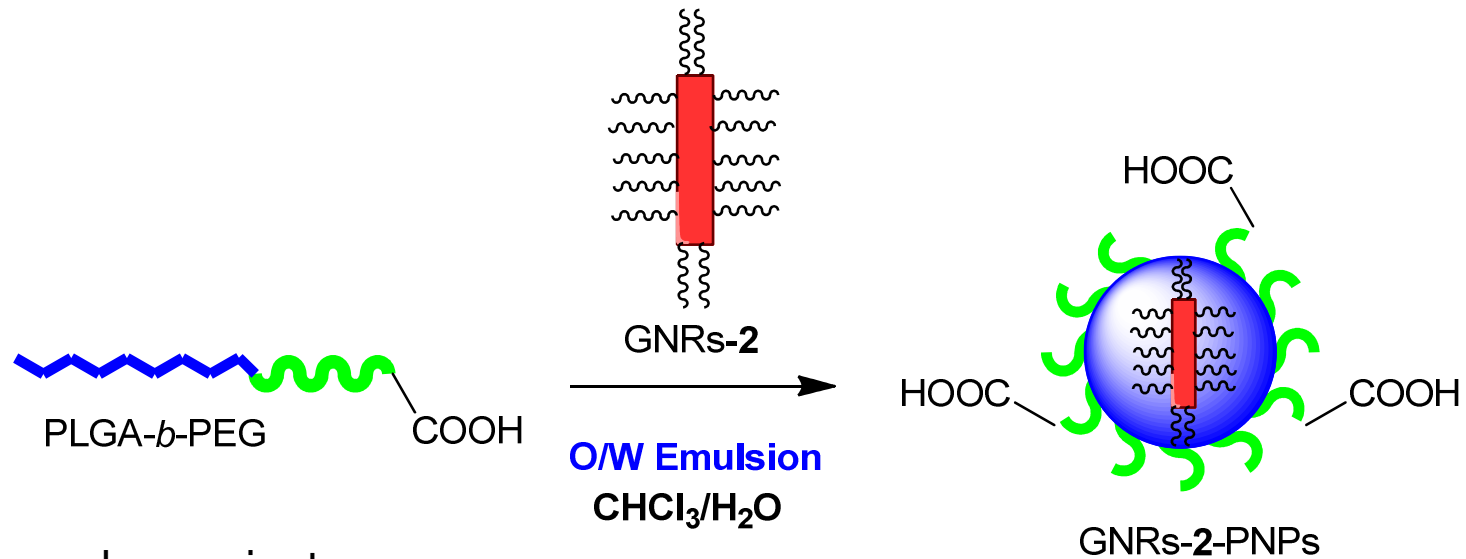




Gold Nanorods (GNRs)



Polymeric nanoparticle's (PNPs) formation



Microtip probe sonicator



Characterization

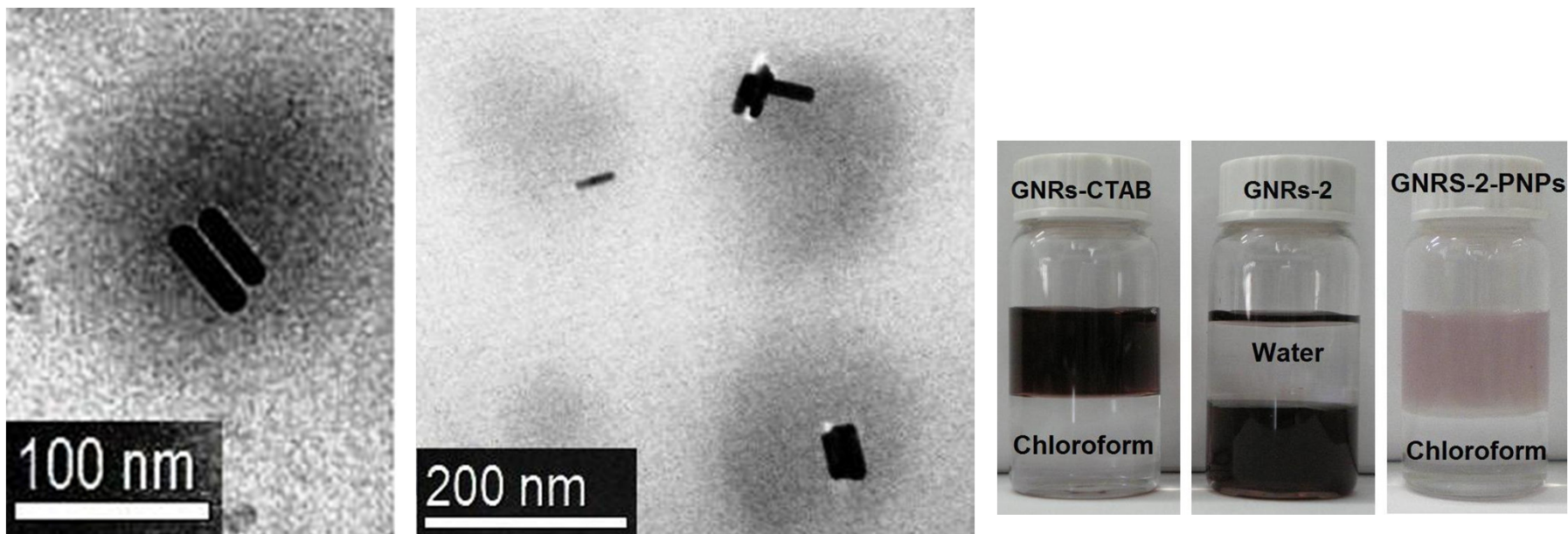
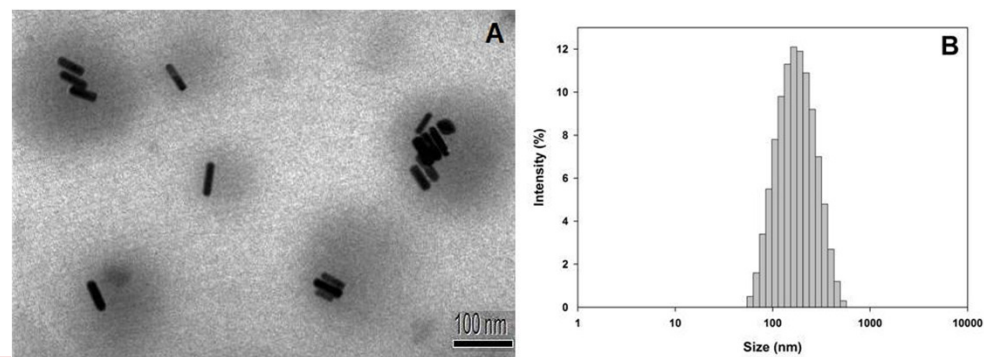


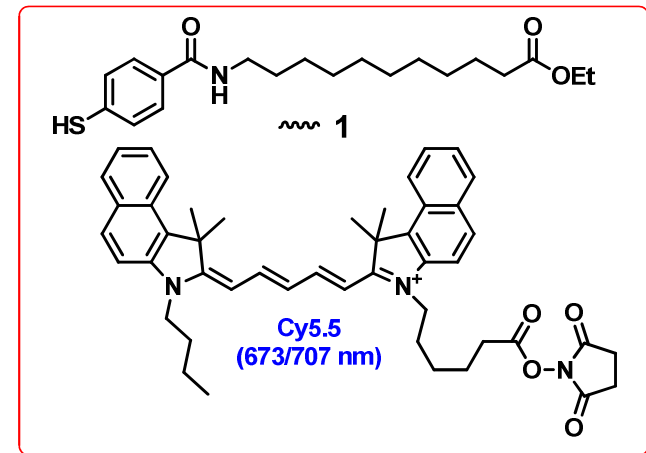
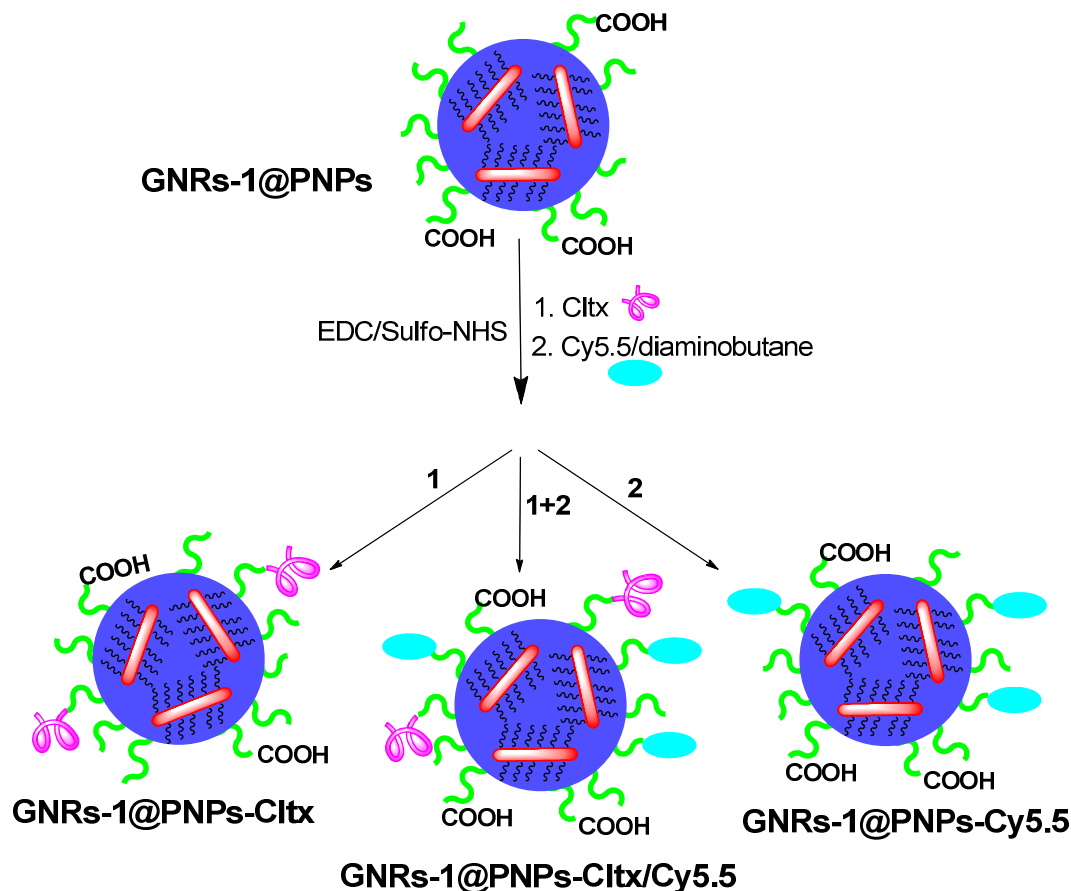
Figure S12. HRTEM of GNRs-2-PNPs.

TEM and DLS



Chlorotoxin-Targeted Polymeric Nanoparticles containing Gold Nanorods: A Theranostic approach against Glioblastoma

Chlorotoxin (Cltx): A specific peptide to target glioma cells
 (MCMPCFTTDHQMARCDDCCGGKGRGKCYGPQCLCR)



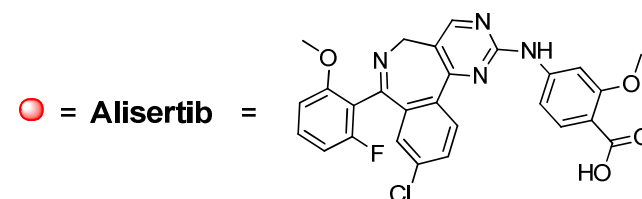
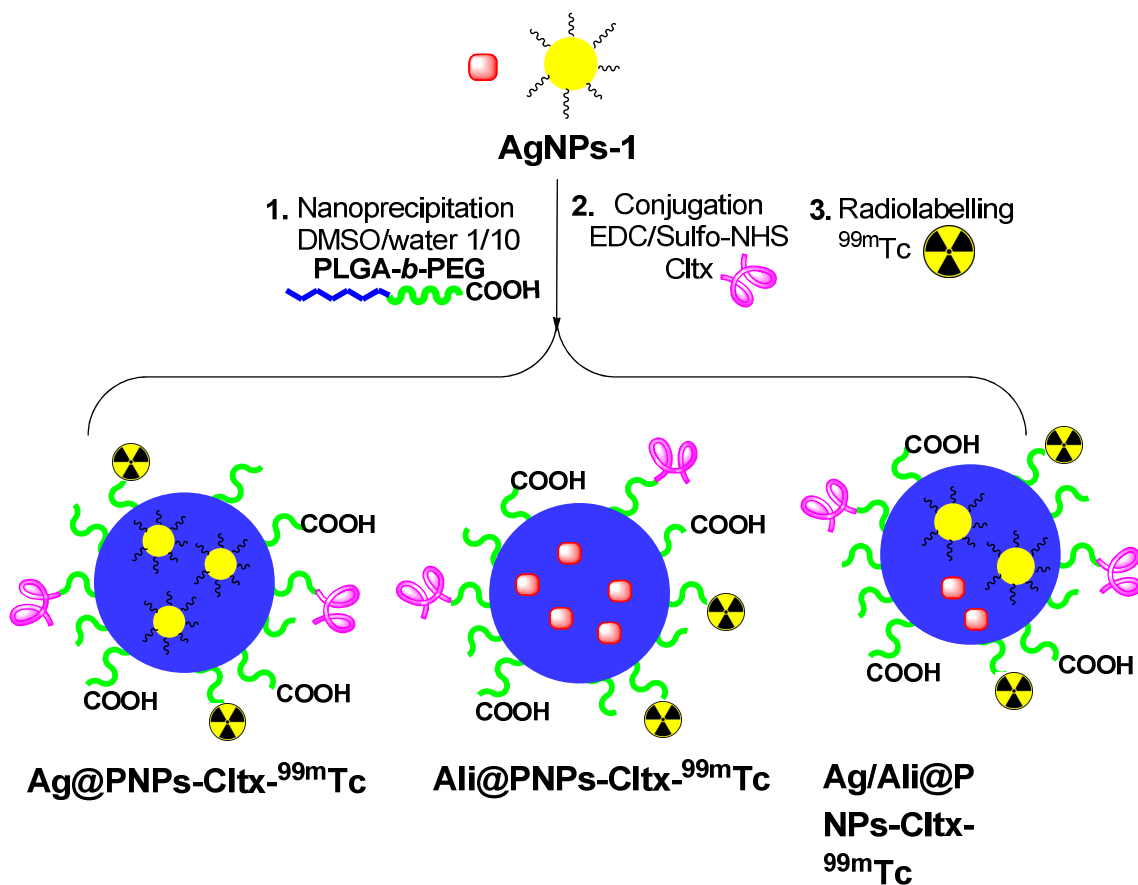
GNRs-1@PNPs-Cltx/Cy5.55

DLS= 122.5 ; ζ -pot.= -26.8 mV;
 [Au]=1200 ppm (6.0 mM)
 [Cy5.5]= 3.2 mM;
 [Cltx]= 125 μ M



Silver Nanoparticles

Targeted Delivery of Silver Nanoparticles and Alisertib. In Vitro and In Vivo Synergistic Effect Against Glioblastoma

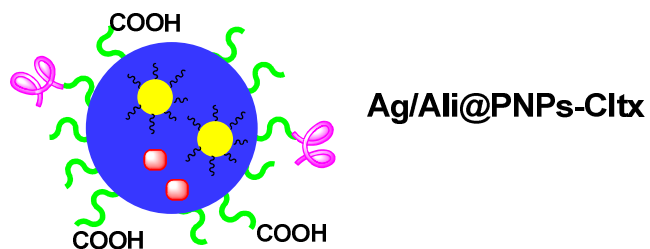


Alisertib has been chosen as pharmacologic model for drug loading since its effect as a selective Aurora A kinase (AAK) inhibitor and its application against solid tumors (epithelial ovarian, fallopian tube and primary peritoneal carcinoma) is well known.

Scheme 1. Synthesis of Ag@PNPs-Cltx- ^{99m}Tc , Ali@PNPs-Cltx- ^{99m}Tc and Ag/Ali@PNPs-Cltx- ^{99m}Tc .



Targeted Delivery of Silver Nanoparticles and Alisertib. In Vitro and In Vivo Synergistic Effect Against Glioblastoma



Ag/Alisertib@PNPs-Cltx

DLS= 130.0 nm, PDI=0.21

ζ -pot.= -16.2 mV;

[Ag]= 2.17 mM

[Alisertib]= 41.8 μ M;

[Cltx]= 100 μ M

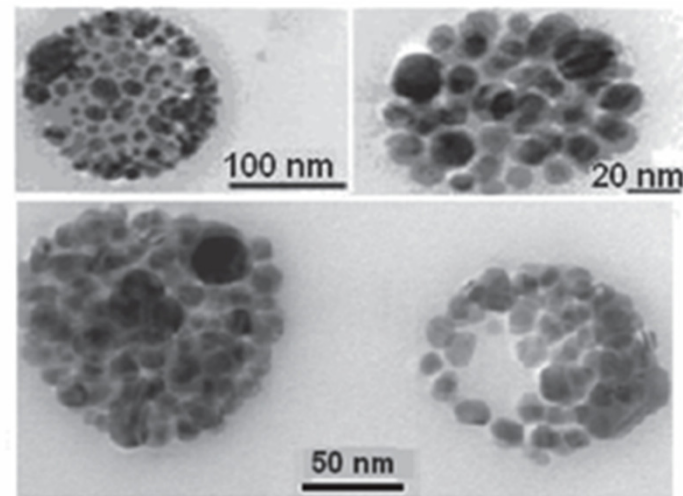


Figure 2. DLS, Z-potential and TEM images for Ag-1-PNPs.



Outline

1. Synthesis of metallic nanoparticles (NPs). Organic ligands to coat the metallic NPs (ligand exchange): lipophilic metallic NPs.

2. Polymeric nanoparticle's (PNPs) formation. Chemical conjugation in the outer shell of the PNPs. The active targeting.

3. Theranostics: *In vitro* and *In vivo* applications.



Magnetic Nanoparticles

M. Comes Franchini, *Langmuir*, **2007**, 4026.

M. Comes Franchini, *Small*, **2010**, 6, 366.

M. Comes Franchini, *Int. J. Nanomedicine*, **2014**, 9, 3037.

In vivo Imaging

Magnetherm apparatus with exchangeable coils and capacitors

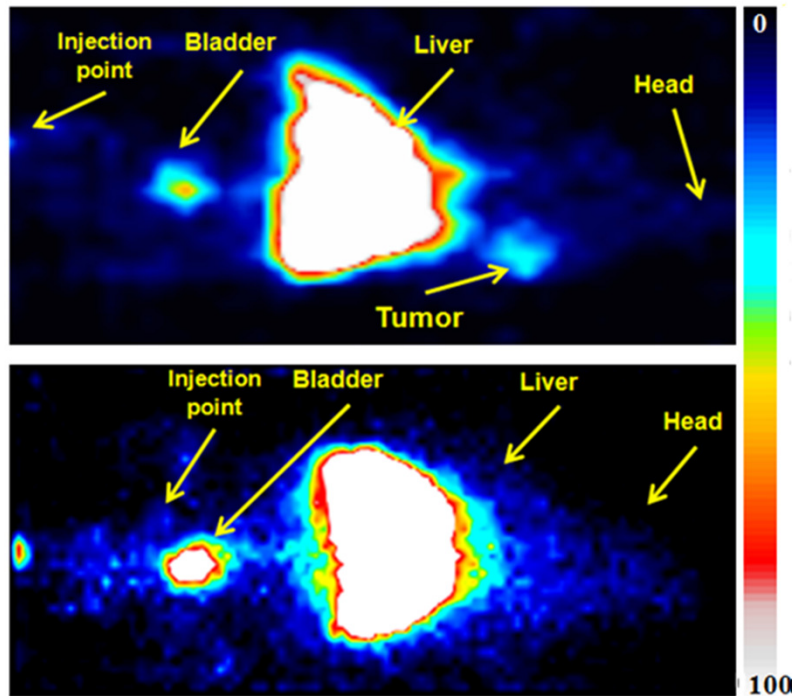
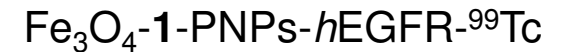
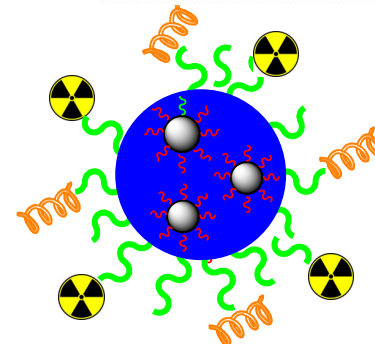


Figure 3. Scintigraphic image of the hybrid radiolabeled Fe_3O_4 -1-PNPs-hEGFR- $^{99\text{m}}\text{Tc}$ in tumour A431bearing scid mouse (up) and the radiolabeled Fe_3O_4 -1-PNPs- $^{99\text{m}}\text{Tc}$ (bottom).

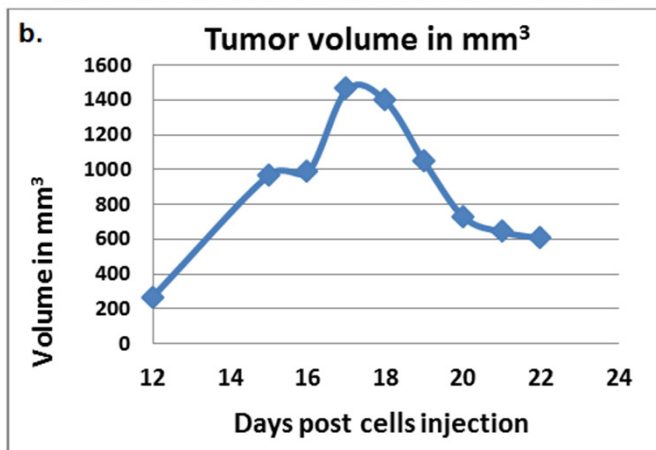
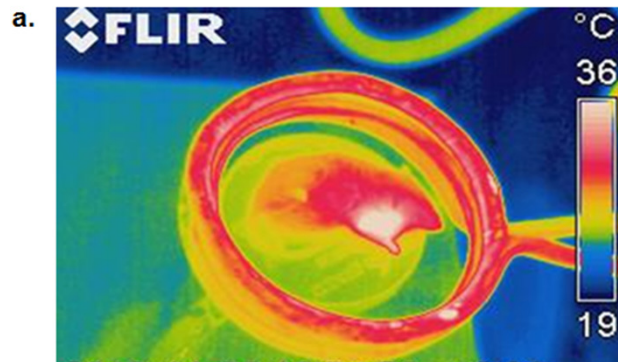


A **significant concentration on the tumor is observed on the left shoulder**, compared to the corresponding muscle tissue on right shoulder, which **is clearly attributed to the EGFR antibody-receptor interaction**.

In collaboration with the *Technological Educational Institute of Athens (Greece)*



In vivo Magnetic Fluid Hyperthermia



Magnetherm apparatus with exchangeable coils and capacitors



Proof of concept experiment for the *in vivo* hyperthermic treatment applied to a mouse model with the above mentioned skin cancer which is the third most common type of all cancers.

To assess the hyperthermia effect, we applied an AMF of $H_0 \sim 25 \text{ kA/m}$, at a frequency of $f = 173 \text{ kHz}$

Temperature monitoring of the mouse being placed inside the coil using an infrared camera. Increased outer temperature on the tumor region is evident. Progress in tumor size: **a noticeable decrease after Day 18 is shown.**

In collaboration with the *Technological Educational Institute of Athens (Greece)*

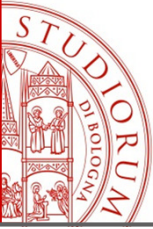


Gold Nanorods (GNRs)

M. Comes Franchini, *Chem. Commun.*, **2009**, 5874.

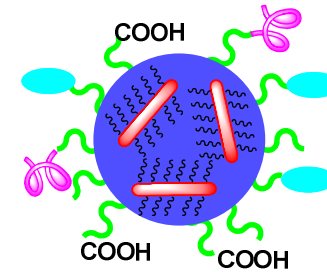
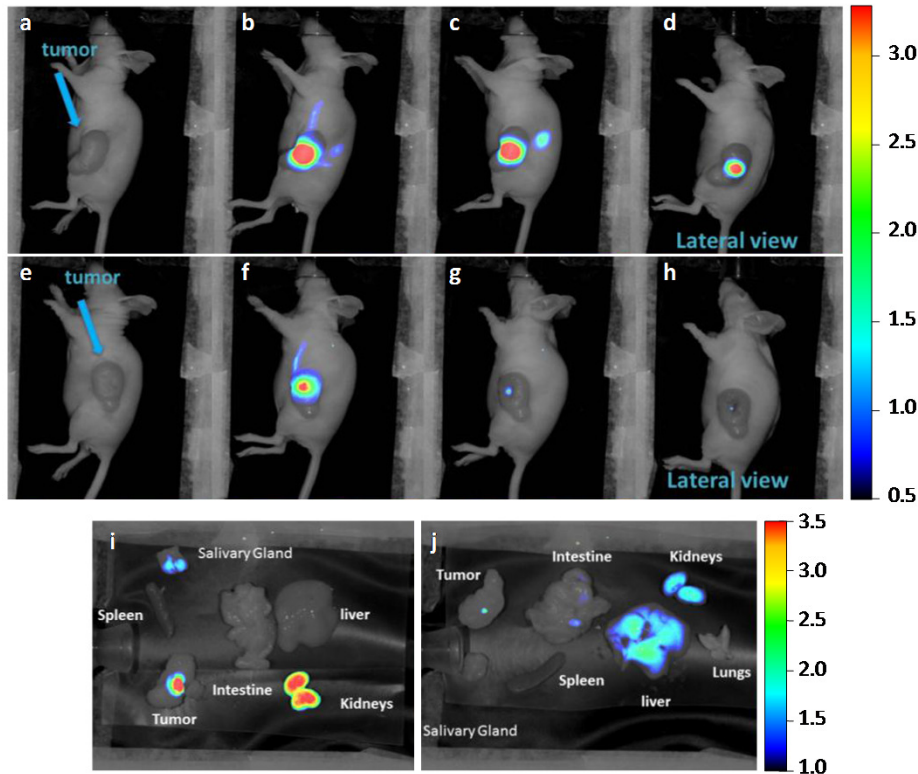
M. Comes Franchini, *J. Mater. Chem.* **2010**, *20*, 10908.

M. Comes Franchini, *J. Nanop. Research.* **2014**, *16*, 2304.



Targeted Polymeric Nanoparticles containing GNRs: A Therapeutic approach against Glioblastoma

In vivo Imaging



GNRs-1@PNPs-Cltx/Cy5.5

Intratumoural administration (0.5 nmol/mouse, 2.5 mL/Kg) in female CD-1 nude mice, which were subcutaneously inoculated with U87MG cells.

For GNRs-1@PNPs-Cltx/Cy5.5, the in vivo signal into the tumour was very intense at 5 min after injection and still persisted at 24 h after injection (Figures 4a-d). A quantitative analysis performed on the fluorescence signal recorded in the tumour of mice after intratumour injection of GNRs-1-PNPs-Cy5.5/Cltx demonstrated that at 4h about 48% of the initial fluorescence was recovered in the tumour and it was still of 22% at 24 h.

Figure 4: Optical Imaging (OI) scans recorded for GNRs-1-PNPs-Cltx/Cy5.5 (a-d) and GNRs-1-PNPs-Cy5.5 (e-h) after intratumour administration in U87MG bearing mouse; i-j: Images recorded on harvested organs and tissues after sacrifice for GNRs-1-PNPs-Cltx/Cy5.5 (i) and GNRs-1-PNPs-Cy5.5 (j).

Collaboration with Ephoran Multi Imaging Solutions (Colleretto Giacosa, Italy).



Silver Nanoparticles

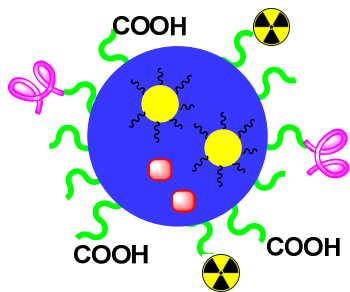
M. Comes Franchini, *Adv. Healthcare Mat.* **2012**, 1, 342.

M. Comes Franchini, *Nanomedicine* **2014**, 9, 839.



Targeted Delivery of Silver Nanoparticles and Alisertib. In Vitro and In Vivo Synergistic Effect Against Glioblastoma

In vivo Imaging



Ag/Ali@PNPs-Cltx-^{99m}Tc

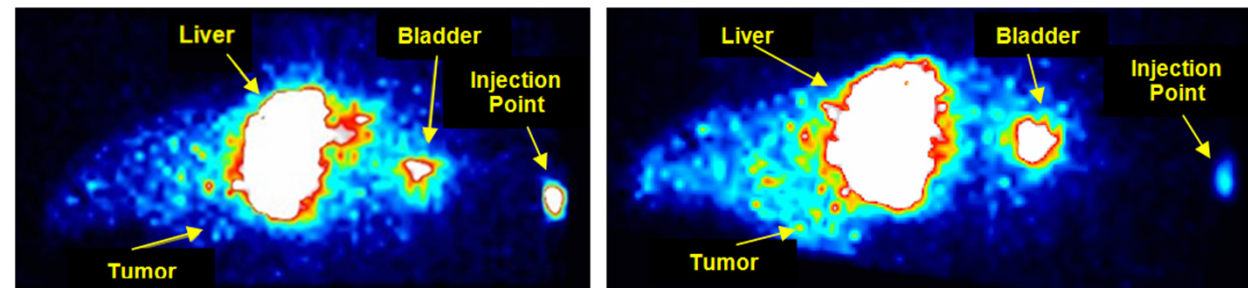
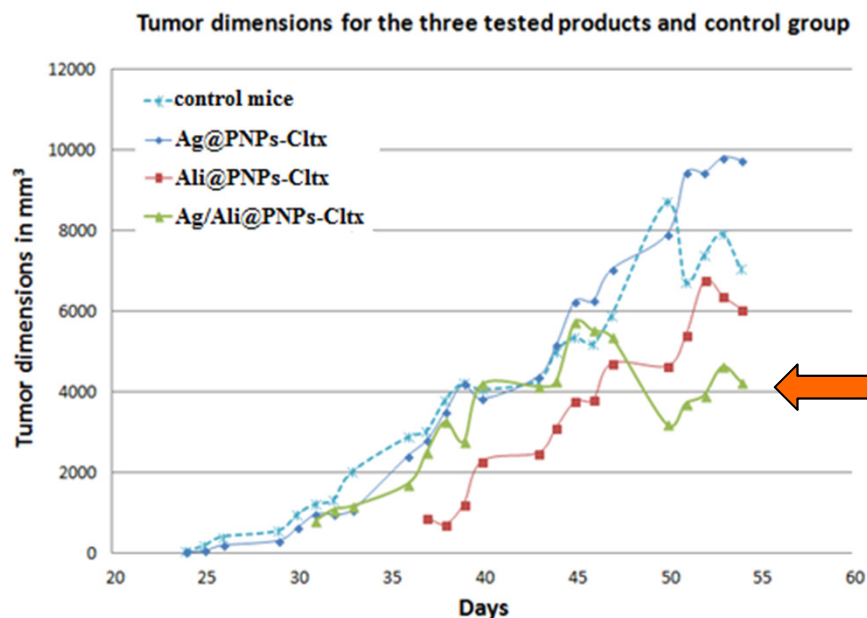


Figure 3. Comparative image of a tumor bearing mouse injected with Ag@PNPs-^{99m}Tc (A) and Ag/Ali@PNP-Cltx-^{99m}Tc (B) p.i.

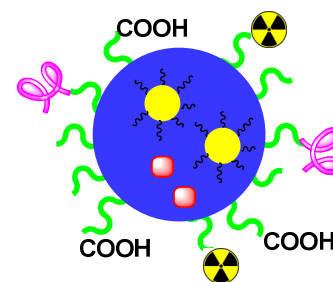
The quantitative analysis on the 2 min. frames shows **a tumor concentration of 0.6% for Ag@PNPs-^{99m}Tc and 5% for Ag/Ali@PNP-Cltx-^{99m}Tc**. This concentration is considered very significant, also compared to normal tissue (< 2%). In addition, concentrations in liver drops from 80% for Ag@PNPs-^{99m}Tc to 60% for Ag/Ali@PNP-Cltx-^{99m}Tc, **therefore the effect of the targeting peptide is quite clear.**

In collaboration with the *Technological Educational Institute of Athens (Greece)*

Targeted Delivery of Silver Nanoparticles and Alisertib. In Vitro and In Vivo Synergistic Effect Against Glioblastoma



In vivo Therapy



Ag/Al@PNPs-Cltx-^{99m}Tc

Figure 4. Tumor dimensions for the four tested mice groups: Control; Ag@PNPs-Cltx; Ali@PNPs-Cltx; Ag/Al@PNPs-Cltx. A decrease in tumor size is observed for Ag/Al@PNPs-Cltx.

Table 1. Comparison between in vitro and in vivo results. In vitro results are expressed as IC50 obtained in U87MG cells after 72 h of incubation; in vivo as decrease in tumor size.

Compounds tested	In vitro in U87MG cells (IC50; μ M)	In vivo in glioblastoma bearing mice (observed decrease in tumour size: average size reduction after day 45)
Ag@PNPs-Cltx	45	+22%
Ali@PNPs-Cltx	0.02	-22%
Ag/Al@PNPs-Cltx	0.01	-34%
Alisertib alone	0.1	n.d.
n.d. not determined		



Magnesium Nanoparticles

Applications: A potential novel green and not-toxic nano-heater

M. Comes Franchini, Chem. Commun. 2014, 50, 7783.

Magnesium Nanoparticles

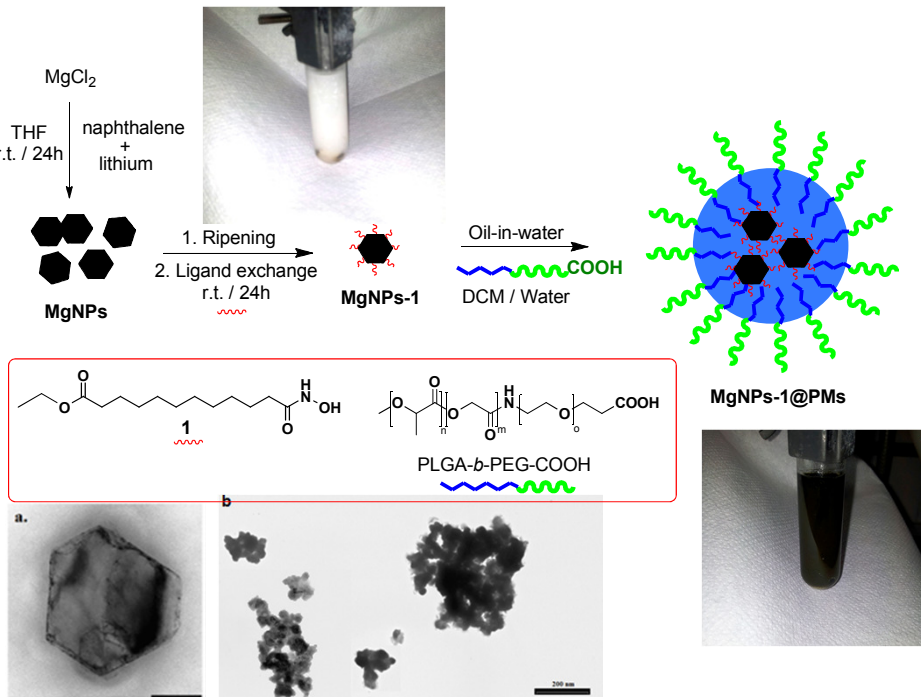


Figure 1: schematic pathway for the synthesis of MgNPs-1@PMs (above). a) TEM image of MgNPs (scale bar 20 nm); b) TEM image of MgNPs-1@PMs (scale bar 200 nm);

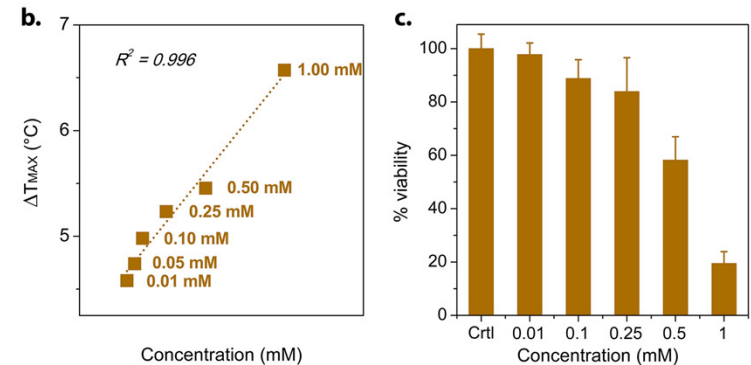
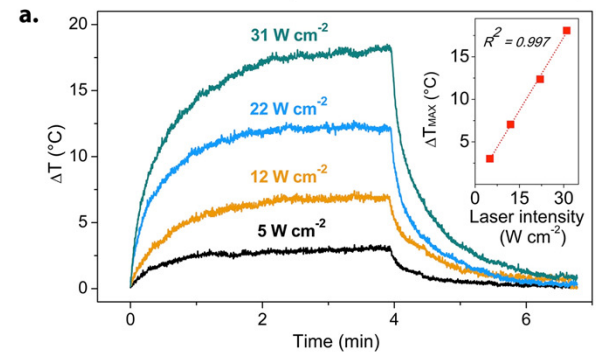


Figure 2: a) temperature profiles obtained by illuminating MgNPs-1@PMs (5.3 mM of Mg) with increasing laser intensities at a fixed $t_{\text{irr}} = 4$ min and diagram of ΔT_{max} increase from (a) vs. laser intensity. b) ΔT_{max} increase versus Mg concentration obtained with a 22 W cm^{-2} laser intensity. c) toxicity evaluation of MgNPs-1@PMs at different concentrations, obtained by Trypan blue exclusion assay.



Acknowledgments



Dr. Erica Locatelli
**Department of Industrial Chemistry «Toso
Montanari», (University of Bologna)**

This work has been partly supported with the funding of the EU-FP7 European project SaveMe (contract number CP-IP 263307-2).